Wear Micro-Mechanisms of Composite WC-Co/Cr - NiCrFeBSiC Coatings. Part II: Cavitation Erosion

D. Kekes[a], P. Psyllaki[a], M. Vardavoulias[b], G. Vekinis[c]

[a]Department of Mechanical Engineering, Technological Education Institute (TEI) of Piraeus, 250 Thivon Avenue and P. Ralli, 122 44, Egaleo, Greece,
[b]PyroGenesis SA, Technological Park of Lavrion, 195 00 Lavrion, Greece,
[c]Department of Materials Science, Demokritos' National Center for Scientific Research, Aghia Paraskevi, 15310 Athens, Greece.

Corresponding author:

P. Psyllaki
Department of Mechanical Engineering,
Technological Education Institute (TEI) of
Piraeus, 250 Thivon Avenue and P. Ralli,
122 44, Egaleo, Greece
E-mail: psyllaki@teipir.gr

A B S T R A C T

Composite coatings with five different proportions of WC-Co/Cr and NiCrFeBSiC components were deposited on stainless steel by HVOF spraying. Cavitation erosion tests were performed and the material removal micro-mechanisms were identified by SEM of both the eroded areas and the specimens' cross-sections. Waves' propagation and deflection at the weak interfaces within the coatings resulted in local tensile stresses perpendicular to the interface direction that eventually led to material removal. Such weak interfaces are the boundaries of the carbide particles with the metal binder within the same splat, those between splats along the same layer and those between successively deposited layers.

© 2014 Published by Faculty of Engineering

1. INTRODUCTION

Metallic mechanical components operating in contact with flowing liquids often face severe wear problems that can reduce drastically their operation lifetime. Local pressure fluctuations, caused from rapid changes in flow or vibrations, lead to generation and subsequent collapse of bubbles within the liquid, a phenomenon referred as cavitation. The shock waves and micro-jets generated during bubble collapse exert intense stress pulses on solid surfaces in the vicinity and the repeated action of these pulses eventually can lead to mechanical material removal from the surface, creating local surface cavities or pits, a phenomenon described as cavitation erosion. Such surface degradation is typical of hydraulic components such as ship propellers, valves, feed water pumps and diesel engines, mostly made of metallic materials.

The erosion aggressiveness on the solid surface depends on both the conversion mechanisms of kinetic to acoustic energy during cavities collapse and micro-bubbles implosion within the liquid, as well as on the properties of the surface itself. With respect to the former issue, several models have been developed to assess the effect

of the potential energy contained in the cavity with the damaging threshold [1]. Mathematical models with respect to the latter issue are targeted in correlating materials cavitation resistance to their mechanical properties, like resistance to plastic deformation and fracture toughness [2]. Cavitation erosion experimental studies commonly involve cumulative material weight loss measurements as a function of testing time. Such weight loss curves for both metallic [3] and ceramic [4,5] materials denote a similar behaviour. They are characterized by an initial stage, commonly referred to as the incubation period, "during which the erosion rate is zero or negligible compared to later stages" [6], followed by a second one characterized by a rapid increase of the weight loss rate.

Metallic components degradation due to cavitation erosion can be alleviated either by hydrodynamic design alterations and/or use of materials with enhanced cavitation erosion resistance. In the latter direction, appropriate surface modification of metallic components has been proposed as an attractive economical and feasible answer, based on the reasonable assumption that "cavitation erosion occurs at the solid/liquid interface" and "only the properties of the surface layer, but not the bulk, contribute to the cavitation erosion resistance of a solid" [7]. For this purpose, both thin and thick coatings deposited by various techniques have been proposed and tested. Examples of the first category include coatings with thickness lower than 12 μm, such as DLC [8], TiN and CrN coatings [9] and Ti/TiN [10] multilayers deposited on steel substrates by cathodic arc evaporation. The second category includes coatings with thickness in the range of 200-400 μm; representative examples are laser-clad Ni-Cr-Fe-WC on brass [7] and Ag plated coatings on steel [11]. However, the vast majority of cavitation erosion resistant thick coatings either metallic, or ceramic, or cermet ones are deposited by thermal techniques [12-21], especially High Velocity Oxyfuel Flame (HVOF) spraying. Each kind of the above coatings possesses its own advantages: metallic ones can be deformed, oxides are relatively hard, exhibiting oxidation resistance and hard carbide-based cermets are characterized by excellent wear resistance under sliding friction conditions.

In specific applications, where wear resistance under both sliding friction and cavitation erosion conditions is required, the elaboration of composite cermet/metal thick coatings could be an appropriate solution. In this perspective, five series of composite coatings, each one containing different proportion of cermet-metal components, prepared by premixing commercially available feedstocks of WC-Co/Cr cermet NiCrFeBSiC metallic powders were deposited on AISI 304 stainless steel substrates by HVOF spraying. Two representative wear conditions were selected for their testing, namely dry sliding friction and cavitation erosion. The wear micro-mechanisms, with respect to the cermet content, under dry sliding friction were analyzed and discussed at the first part of this work [22]. The present study aims to further elucidate the wear behaviour and material removal micro-mechanisms under cavitation erosion regime.

2. EXPERIMENTAL PROCEDURE

The same five series of HVOF composite coatings, described in the first part [22], were used in this work. Square specimens of approximately 30×30 mm were sectioned from the as-sprayed samples and polished to a final average roughness (R_a) of 0.5±0.1 μm, since the value of the as-deposited ones was relatively high for surface testing. Erosion tests were performed using a vibratory cavitation apparatus, operating at 20 kHz and 30 μm peak-to-peak amplitude, a sketch of which is shown in Fig. 1. The specimens were held in a rigid stainless steel jig attached to the ultrasonic titanium alloy anvil, immersed 50 mm below the free surface of a fresh charge of distilled water maintained at 20±2 °C, as described previously [4]. The polished surface was positioned 1±0.1 mm from the horn tip, an arrangement that resulted in a circular erosion area with a diameter of 1.4 mm (Fig. 2).

Even though the relevant ASTM G32 "Standard Test Method for Cavitation Erosion Using Vibratory Apparatus" specification requires interrupted testing of the same specimen to determine the cumulative mass loss, in the present study different specimens were tested in one hour intervals from 1 up to a maximum duration of 10 h, in order to visualise the wear micro-mechanisms evolution via post-testing

microscopic observations on their cross-sections. After each test, the specimens were dried at 120 °C for 2 h, then weighed using an analytical balance with an accuracy of 10^{-4} g and stored for further examination.
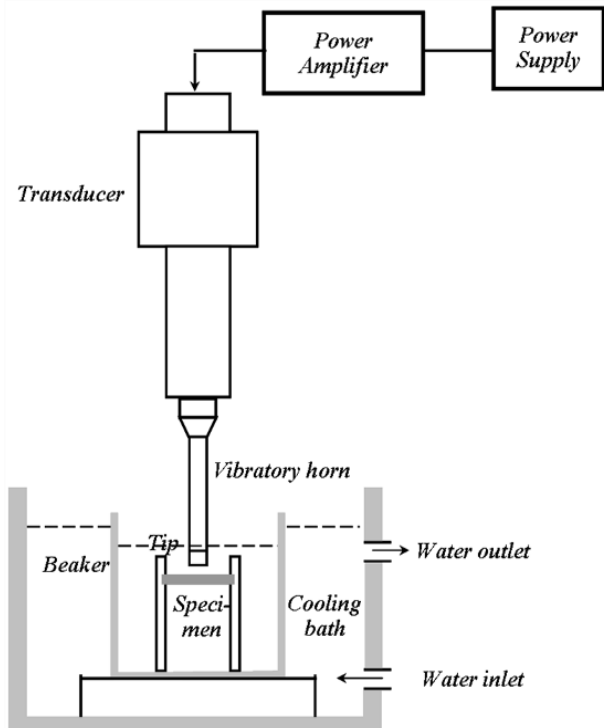

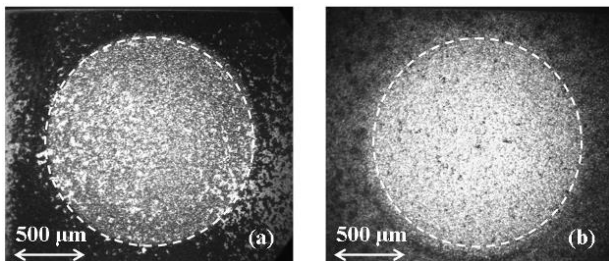**Fig.1.** Cavitation erosion experimental assembly.

Fig. 2. Typical top view appearance of the eroded surface after 5 (a) and 10 (b) hours of testing (Stereo-photographs, 50 % WC-Co/Cr).

Macroscopic observations of the eroded surfaces were performed with a Leica MS 5 stereoscope. Microstructure characterisation and elemental micro-analysis were conducted with the aid of an FEI XL40 SFEG Scanning Electron Microscope (SEM) equipped with an Energy Dispersive X-ray Spectrometry (EDS) detector. In contrast to most relevant studies on cavitation erosion of coatings which involve SEM observation of the eroded surface only, in the present study such characterization was performed in addition on the coatings' cross-sections after exposure. Prior to SEM observations of the cross-sections of the

eroded specimens, special attention was paid for the metallographic preparation, in order to avoid insertion of secondary defects. First, the specimens were carefully sectioned using diamond and SiC cutting wheels, for the cermet coating and the metallic substrate, respectively. The cross-sections were cold mounted under vacuum using an impregnation resin suitable for the observation of open pores and cracks.

3. RESULTS

Detailed microstructure and phase composition analyses of the as-sprayed coatings have been presented in the first part of the work [22].

In the case of the metallic-only coating, i.e. 0 % WC-Co/Cr, typical SEM micrographs of the cross-sections of the eroded coating after one, five and ten hours of testing are presented in the left column of Fig. 3. Details of each cross-section in higher magnifications are shown in the right column of the same figure. From the sequence of these "snapshots" the evolution of the material removal mechanism can be inferred.
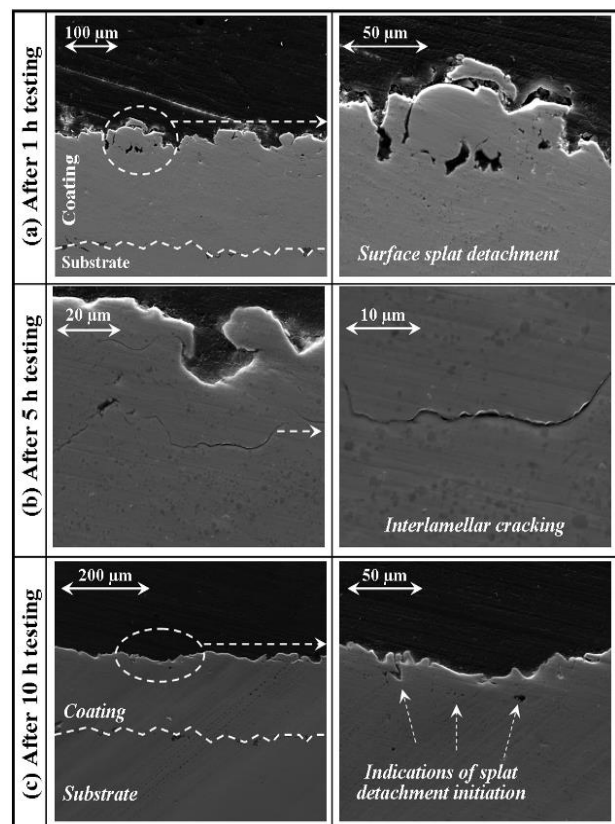

Fig. 3. Evaluation of the cavitation erosion mechanism of the 0 % WC-Co/Cr coatings (SEM micrographs of cross-sections).

The impact of the bubbles on the coating surface causes the local creation of micro-voids at the splat boundaries of the top (outmost) lamella (Fig. 3a). The eventual growth and coalescence of these voids induces a splat-by-splat exfoliation mechanism at the same surface lamella level. The inherent ductility of the metallic phase has resulted in local plastic deformation at the rims around the craters remaining after splat exfoliation (Fig. 3b). Even though, in parallel, sub-surface erosion effects are taking place, their magnitude becomes obvious only after longer testing times. For example in Fig. 3b, in addition to cracking along the surface splats boundaries, a sub-surface crack at a depth of ~35 μm from the exposed surface can be clearly observed. Such sub-surface cracks can be correlated to the coating's interfacial roughness, since they are always located at the interlamellar boundaries between successive lamellae, propagating along them. The splat-by-splat exfoliation wear micro-mechanism, together with lamella-by-lamella successive removal leads in later stages to visible reduction of the coatings thickness. For example, for the particular coating (Fig. 3c) this reduction is about 60 μm after ten hours of testing, corresponding approximately to the removal of four lamellae layers. The above described synergistic mechanisms are continued throughout the test duration, leading to the removal of the each time exposed top layer, via micro-voids creation and coalescence around the splat boundaries.

From the SEM photographs of the cross-section of the ceramic-only coating, i.e. 100 % WC-Co/Cr, eroded for 5 h (Fig. 4) can be concluded that, also in this case, erosion leads to the removal of entire surface particles, corresponding, for example, to the created crater enclosed within the dotted circle (b) in Fig. 4a. Higher magnifications helped to reveal additional sub-surface damage of the coating, extending to depths even at distances corresponding to its half-thickness. Areas just underneath the craters (Fig. 4b) are characterized by cracks propagating around the splat boundaries, whereas at areas more remote from the surface (Fig. 4c) cracks parallel to the coating/ substrate interface extending between successive lamellae can be also clearly distinguished.
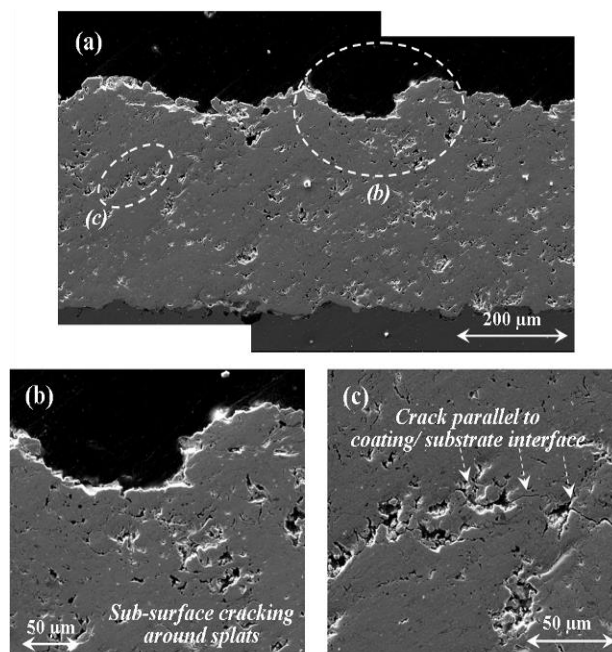

Fig. 4. (a) SEM micrographs of cross-sections of the 100 % WC-Co/Cr coating after 5 h testing, (b) and (c) magnifications of the respective marked areas in (a).

SEM observations of the eroded surface of this coating at earlier testing stages (2 h), shown in Fig. 5, help in identifying the material removal micro-mechanisms. Cavitation craters with diameters of the order of ~100 μm are clearly visible between un-removed splats, corresponding approximately to the dimensions of the solidified particles (Fig. 5b). Similar observations have been reported in cavitation erosion studies on WC-17Co cermet HVOF coatings [19]. This is indicative of rupture of the interface between adjacent splats, inducing inter-splat fracture and, consequently, whole-splat removal. Moreover, higher magnification at the scale of a splat revealed the existence of intra-splat, circular-like micro-pores (Fig. 5c), of diameters about 1-2 μm. As shown in Fig. 5d, this porosity can be correlated to carbide particles expulsion from the metal binder matrix (Fig. 5d).

A typical SEM photograph of a cross-section of the composite coating (50 % WC-Co/Cr) tested for 5 h is shown in Fig. 6. In this case, wear is characterized by the detachment of an entire surface lamella. This detachment is due to the propagation of a crack extending within the metallic phase and following the interfacial roughness of the stratified coating structure. The relevant SEM photographs, together with local EDS microanalysis on characteristic areas of the eroded surface are shown in Fig. 7.
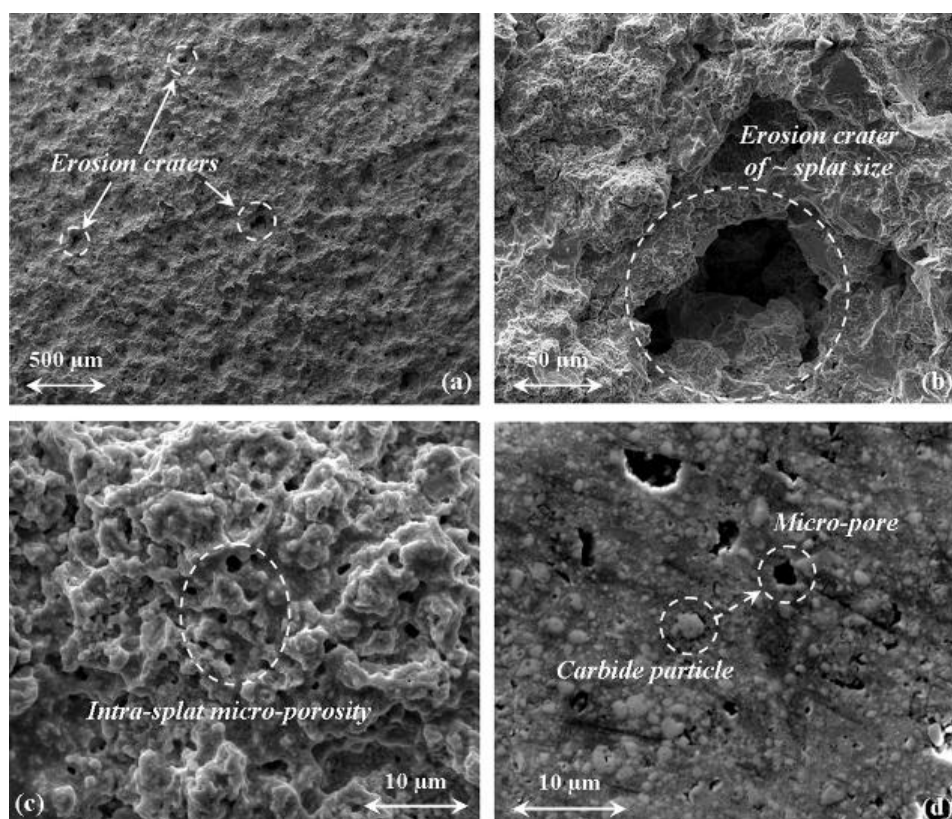
Fig. 5. (a) SEM top-view micrograph of the eroded surface of the 100 % WC-Co/Cr coatings, after 2 h testing, (b), (c) and (d) successive magnifications of (a).
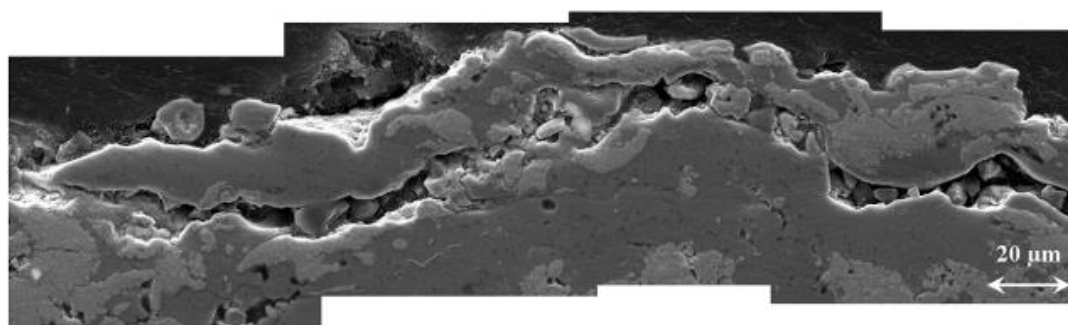

Fig. 6. SEM cross-section of the 50 % WC-Co/Cr composite coating, after 5 h cavitation erosion testing.

On a metallic non-removed surface splat, small craters of dimensions around 400 nm with traces of plastic deformation around their rims can be observed (Fig. 7b).

The ceramic ones are characterized by the existence of a denser network of craters, of larger dimensions corresponding to the size of the carbide particles, as previously described (Fig. 7c).

In Fig. 8, the cumulative weight loss for the five coatings as a function of testing time, measured according to the ASTM G32 specification, is shown. In the literature [3,4,8,14] such graphs

aid to the identification of the successive stages –incubation, acceleration, deceleration- of surface material removal under ultrasonic vibration conditions. In the present case, a much higher material removal rate is observed in the case of the purely cermet coating, whereas the wear rates of the composite ones are closer to that of the purely metallic coating. Even though the much higher weight loss values in the case of cermet-only coatings are partially due to the large difference between the specific gravities of the cermet and metallic phase, this finding is nevertheless a clear indication that the metallic NiCrFeSiBC phase decelerates the removal of cermet phase.
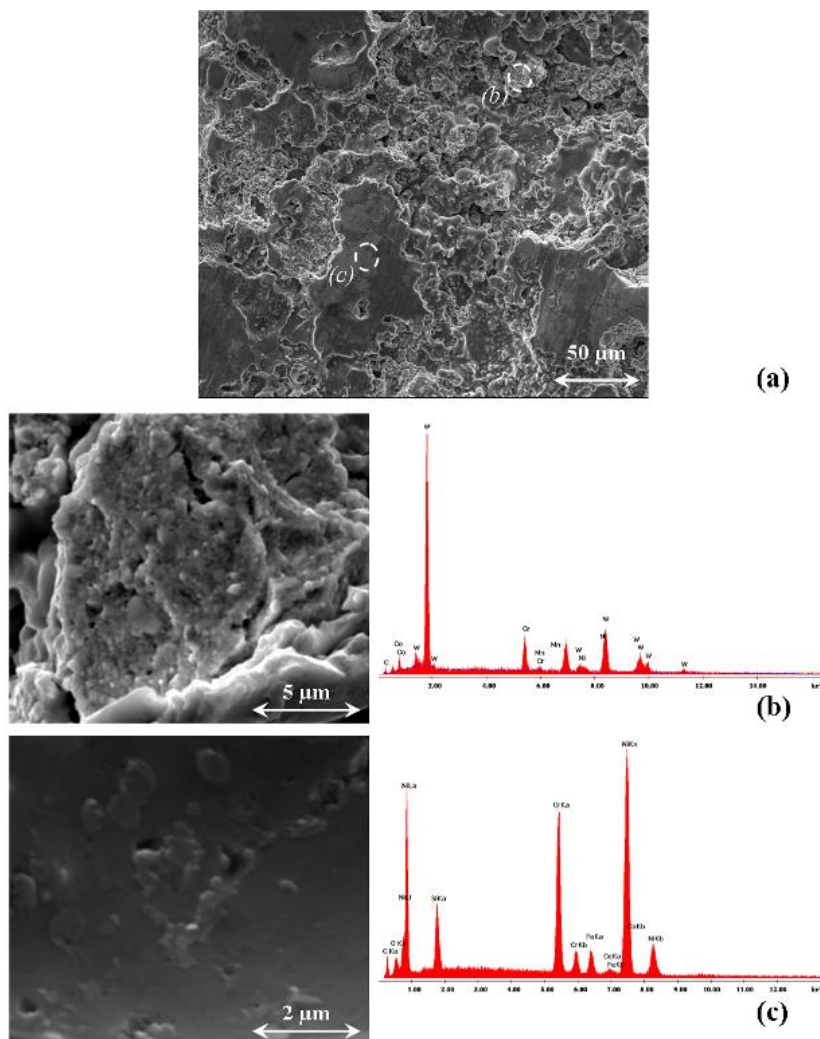
Fig. 7. (a) Typical SEM top-view micrographs of 50 %WC-Co/Cr composite coating, after 5 h testing, (b) and (c) magnifications and local EDS microanalysis in respective areas marked in (a).
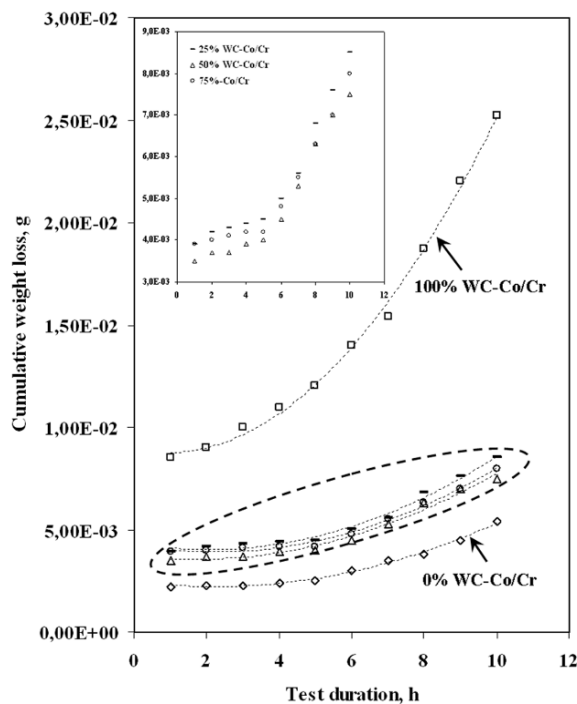

Fig. 8. Cumulative weight loss of all coating series as a function of cavitation erosion testing time.

4. DISCUSSION

A common feature in all the coating systems studied was that failure was not limited only to the outmost exposed surface, but it extended to a significant distance underneath it, within the coating volume. The essential characteristic of this mode of failure is that always occurred at interfaces associated with coatings' structural discontinuities. In the present case of stratified coatings, such discontinuities can be categorized as follows:

- These encountered within a single splat between phases of significantly different properties, e.g. carbide particles dispersed in the metallic binder phase.

- Boundaries between adjacent splats of the same layer, either metallic or cermet ones, co-deposited during spraying.

- Boundaries between successively deposited lamellar layers, creating a non-planar "interfacial roughness".

The acoustic waves created at the exposed surface during the bubbles' impact are subsequently propagating within the solid with a velocity depending on the acoustic impedance of the material [23]. At loci where alteration of materials' impedance takes place, a component of the wave is subjected to reflection whereas the rest continues its transmission, their relevant ratio depending on the materials' acoustic properties. The reflected and the transmitted components, propagating in opposite directions, induce local displacements and therefore a tensile stress field on each particular interface. It should be mentioned here that as-sprayed coatings are not entirely free of micro-porosity due to their deposition process consisting of splat-by-splat and layer-by-layer stratified solidification. Such regions of micro- (or even nano-) porosity can act as crack initiation points, should the stress exceed a critical value. Eventually final failure of an interface during testing occurs due to multiple oscillations of the resulted displacements, as the crack previously initiated is now propagating along the path of minimum energy.

Micro-pores and/ or un-melted particles within the coatings structure have been indicated by several other studies as detachment initiation areas [13,15-17,20,21]. The role of coatings porosity on erosion resistance has been clearly pinpointed in [17], where conventional and nano-grain WC-10Co-4Cr feedstock powders were employed for the deposition of HVOF coatings on stainless steel. The lower porosity of the coatings obtained with the nano-powders was directly related to their higher cavitation erosion resistance compared to that of the coatings obtained with conventional powders.

As a particular wave is propagating across the coating, its transmitted component attenuates since a percentage is back-reflected at each interface. However, in the other hand, with the advancement of testing and as material is removed, a particular inner interface is "shifted" closer to the exposed surface, therefore subjected to higher stresses levels, with its actual cohesion strength depending on its prior "damage history". Such a fatigue mechanism can be responsible for both the severity of phenomena occurring at the surface layer and their existence along a non-negligible sub-surface distance, as well as for the specific failure features observed at the different kinds of interfaces, mentioned above:

- In the case within a single surface cermet splat, carbide particles are distributed within the metallic binder phase of drastically different acoustic impedance. Therefore, the stresses created due to the waves' reflection at the carbide/ metal boundaries result in carbide exfoliation (Fig. 5d).

- In the case of adjacent splats of the same surface layer, due to the same cause, micro-pores at the splat-by-splat boundaries are "enlarged", becoming thus visible even at the earlier testing stages. During the testing advancement, these pores grow and eventually coalesce, leading to the final entire splat exfoliation. This micro-mechanism is clearly distinguishable especially in the case of metallic-only coatings, i.e. 0 % WC-Co/Cr (Fig. 3a), since the metal can assume plastic deformation without being fractured and removed.

- Waves' propagation leads to lamellae decohesion, even at subsurface areas, where cracks are initiated and propagating along lamellae interfaces with their profiles typically following the roughness of the

metallic substrate (Fig. 3b and 4c). This interfacial fracture, as expected, is more intensive closer to the exposed surface. The progress of such a micro-mechanism leads to the final removal of entire lamellae, reducing the coating thickness. For example, an entire decohered surface lamella just prior to removal is clearly visible in the case of 50 % WC-Co/Cr (Fig. 6).

It is worth mentioning that for that all types of coatings, cavitation erosion testing led to fracture of interfaces, without any evidence of trans-splat crack propagation, irrelevant to their nature, i.e. metallic or cermet.

Based on the above, it could be assumed that in these particular coatings, the incubation period recorded is the overall time needed for internal flaws to initiate, propagate and induce a measurable weight loss of the removed entities: carbide particle, splat or lamella. These flaws nevertheless affect the coating integrity upon their creation and can, under special circumstances, activate secondary failure modes. It is therefore essential to understand the fundamental wear micro-mechanisms taking place in different materials or structures, so that suitable evaluation methods [24] can be selected and the quantitative results can be properly interpreted.

5. CONCLUSIONS

The cavitation erosion micro-mechanisms of WC-Co/Cu - NiCrFeBSiC composite coatings developed by HVOF spraying onto AISI 304 stainless steel were studied by Scanning Electron Microscopy of the eroded surfaces, as well as of the relevant specimens' cross-sections. Two main conclusions common for all the coating systems studied can be drawn. In the one hand failure was not limited only to the outmost exposed surfaces, but extended to a significant distance underneath them. In the other hand cavitation erosion led to fracture of interfaces, without any evidence of trans-splat crack propagation. Acoustic waves generated at the exposed surface of the tested materials are propagating across the coating thickness, through multiple partial reflections at interfaces associated with the coatings structural discontinuities. The local tensile stress fields

thus induced result in micro-pores initiation, growth and coalescence, as well as crack initiation and propagation along the inner "weak" boundaries of the stratified layers.

The overall material removal mechanism can be considered as a superposition of carbide particles exfoliation at the level of a single cermet splat, splat exfoliation at the level of the outmost lamella exposed to erosion, and finally of entire surface lamella de-cohesion from the layers underneath. In the case of composite coatings, the metallic phase was found to retard erosion wear.

These findings, together with those reported in the first part of this work on the sliding wear micro-mechanisms of the same series of coatings can help in elucidating the wear behavior of randomly stratified cermet-metallic coatings, exposed to various wear regimes.

REFERENCES

[1] T.J.C. Van Terwisga, P.A. Fitzsimmons, L. Ziru, E. Jan Foeth:, *Cavitation Erosion–A review of physical mechanisms and erosion risk models*, Proceedings of the 7th International Symposium on Cavitation CAV2009, 16-20.08.2009, Ann Arbor/ Michigan, USA Paper No 41.

[2] M. Szkodo: *Mathematical description and evaluation of cavitation erosion resistance of materials*, Journal of Materials Processing Technology, Vol. 164-165, pp. 1631-1636, 2005.

[3] M.C. Park, G.S. Shin, J.Y. Yun, J.H. Heo, D.I. Kim, S.J. Kim: *Damage mechanism of cavitation erosion in austenite→martensite phase transformable Fe-Cr-C-Mn/Ni alloys*, Wear, Vol. 310, No. 1-2, pp. 27-32, 2014.

[4] W.J. Tomlinson, N. Kalitsounakis, G. Vekinis: *Cavitation erosion of aluminas*, Ceramics International, Vol. 25, No. 4, pp. 331-338, 1999.

[5] B. Karunamurthy, M. Hadfield, C. Vieillard, G. Morales: *Cavitation erosion in silicon nitride: Experimental investigations on the mechanism of material degradation*, Tribology International, Vol. 43, No. 12, pp. 2251-2257, 2010.

[6] Y. Meged: *Modeling of the initial stage in vibratory cavitation erosion tests by use of a Weibull distribution*, Wear, Vol. 253, No. 9-10, pp. 914-923, 2002.

[7] K.F. Tam, F.T. Cheng, H.C. Man: *Cavitation erosion behavior of laser-clad Ni-Cr-Fe-WC on brass*, Materials Research Bulletin, Vol. 37, No. 7, pp. 1341-1351, 2002.

[8] F. Cheng, S. Jiang: *Cavitation erosion resistance of diamond-like carbon coating on stainless steel*, Applied Surface Science, Vol. 292, pp. 16-26, 2014.

[9] A. Krella: *Cavitation erosion of TiN and CrN coatings deposited on different substrates*, Wear, Vol. 297, No. 1-2, pp. 992-997, 2013.

[10] A.K. Krella: *Cavitation erosion resistance of Ti/TiN multilayer coatings*, Surface and Coatings Technology, Vol. 228, pp. 115-123, 2013.

[11] S. Hattori, K. Taruya, K. Kikuta, H. Tomaru: *Cavitation erosion of silver plated coatings considering thermodynamic effect*, Wear, Vol. 300, No. 1-2, pp. 136-142, 2013.

[12] S.A. Romo, J.F. Santa, J.E. Giraldo, A. Toro: *Cavitation and high-velocity slurry erosion resistance of welded Stellite 6 alloy*, Tribology International, Vol. 47, pp. 16-24, 2012.

[13] W. Yuping, L. Pinghua, C. Chenglin, W. Zehua, C. Ming, H. Junhua: *Cavitation erosion characteristics of a Fe-Cr-Si-B-Mn coating fabricated by high velocity oxy-fuel (HVOF) thermal spray*, Materials Letters, Vol. 61, No. 8-9, pp. 1867-1872, 2007.

[14] K. Jafarzadeh, Z. Valefi, B. Ghavidel: *The effect of plasma spray parameters on the cavitation erosion of Al_2O_3-TiO_2 coatings*, Surface and Coatings Technology, Vol. 205, No. 7, pp. 1850-1855, 2010.

[15] Y. Wu, S. Hong, J. Zhang, Z. He, W. Guo, Q. Wang, G. Li: *Microstructure and cavitation erosion behavior of WC-Co-Cr coating on 1Cr18Ni9Ti stainless steel by HVOF thermal spraying*, International Journal of Refractory Metals and Hard Materials, Vol. 32, pp. 21-26, 2012.

[16] S. Hong, Y. Wu, Q. Wang, G. Ying, G. Li, W. Gao, B. Wang, W. Guo: *Microstructure and cavitation-silt erosion behavior of high-velocity oxygen-fuel (HVOF) sprayed Cr_3C_2-NiCr coating*, Surface and Coatings Technology, Vol. 225, pp. 85-91, 2013.

[17] L. Thakur, N. Arora: *A study on erosive wear behavior of HVOF sprayed nanostructured WC-CoCr coatings*, Journal of Mechanical Science and Technology, Vol. 27, No. 5, pp. 1461-1467, 2013.

[18] H.S. Grewal, H. Singh, A. Agrawal: *Understanding Liquid Impingement erosion behaviour of nickel-alumina based thermal spray coatings*, Wear, Vol. 301, No. 1-2, pp. 424-433, 2013.

[19] G. Hou, X. Zhao, H. Zhou, J. Lu, Y. An, J. Chen, J. Yang: *Cavitation erosion of several oxy-fuel sprayed coatings tested in deionized water and artificial seawater*, Wear, Vol. 311, No. 1-2, pp. 81-92, 2014.

[20] J.F. Santa, L.A. Espitia, J.A. Blanco, S.A. Romo, A. Toro: *Slurry and cavitation erosion resistance of thermal spray coatings*, Wear, Vol. 267, No. 1-4, pp. 160-167, 2009.

[21] J. Lin, Z. Wang, P. Lin, J. Cheng, X. Zhang, S. Hong: *Microstructure and cavitation erosion behavior of FeNiCrBSiNbW coating prepared by twin wires arc spraying process*, Surface and Coatings Technology, Vol. 240, pp. 432-436, 2014.

[22] D. Kekes, P. Psyllaki, M. Vardavoulias: *Wear micro-mechanisms of composite WC-Co/Cr - NiCrFeBSiC coatings. Part I: Dry sliding, Tribology in Industry, Vol. 36, No. 4, pp. 361-374, 2014.*

[23] G. Rosa, P. Psyllaki, R. Oltra, S. Costil, C. Coddet: *Simultaneous laser generation and laser ultrasonic detection of the mechanical breakdown of a coating-substrate interface*, Ultrasonics, Vol. 39, No. 5, pp. 355-365, 2001.

[24] M. Gäkle, M. Kley, L. Ritzel: *Cavitation tests to materials and coatings - Comparison of different evaluation processes and identification of the cavitation erosion of EN-GJS-600-3, G-CuAl8Mn8 and GX4CrNi13-4 + QT*, Materialwissenschaft und Werkstofftechnik, Vol. 44, pp. 774-782, 2013 (in German).